

# Dust in the Radio Galaxy and Merger Remnant NGC 1316 (Fornax A)

B D Asabere<sup>1</sup>, C Horellou<sup>2</sup>, H Winkler<sup>1</sup> and L Leeuw<sup>3</sup>

<sup>1</sup> Department of Physics, University of Johannesburg, C1-Lab, P.O. Box 524, 2006, Auckland Park, Johannesburg, South Africa

<sup>2</sup> Department of Earth & Space Sciences, Chalmers University of Technology, Onsala Space Observatory, SE-439 92 Onsala, Sweden

<sup>3</sup> Department of Interdisciplinary Research, University of South Africa, P.O.Box 392, UNISA, 003, South Africa

E-mail: [bd.asabere@gmail.com](mailto:bd.asabere@gmail.com)

**Abstract.** We present dust maps of NGC 1316 (Fornax A), a well-studied early-type galaxy located in the outskirts of the Fornax cluster. We used the Large APEX BOLometer CAmera (LABOCA), operating at  $870\ \mu\text{m}$  with an angular resolution of  $19.''5$  on the Atacama Pathfinder EXperiment (APEX) 12 m submillimeter telescope in Chile and the Wide-field Infrared Survey Explorer (WISE). WISE observed in four mid-infrared bands centered at 3.4, 4.6, 12 and  $22\ \mu\text{m}$  with angular resolutions ranging from 6 to  $12''$ . The WISE and LABOCA maps reveal emission from dust in the central  $2'$  of NGC 1316. The disturbed optical morphology with many shells and loops, the complex distribution of molecular gas and our dust maps are evidences of past merger activity or gas accretion in the galaxy. Combining the LABOCA flux measurement with existing mid- and far-infrared measurements, we estimate the temperature of the cold ( $\sim 22\ \text{K}$ ) and warm ( $\sim 55\ \text{K}$ ) dust components in NGC 1316. This study will be extended to other southern radio galaxies and merger remnants. Those galaxies are good targets for future observations at higher angular resolution and sensitivity with ALMA to probe the interaction of the radio jets with the dusty molecular gas near active galactic nuclei.

## 1. Introduction

Dust is ubiquitous in the interstellar medium (ISM) of galaxies but it constitutes only about 1% of the total mass of the ISM. Notwithstanding, dust plays an important role in galaxies: it is a tracer of star formation and stellar evolution, and contributes to the evolution of galaxies [1, 2]. Interstellar dust grains span a wide range of sizes ( $\sim 0.001$ – $0.25\ \mu\text{m}$ ) and temperatures ( $\sim 20$ – $200\ \text{K}$ ). Dust causes extinction of starlight: it dims and reddens the galaxy light at ultraviolet (UV) and optical wavelengths, but re-radiates about 90% of the absorbed galaxy energy into the infrared and submillimeter wavebands. Interstellar dust can thus be observed in different galactic environments by mapping the re-radiated emission at mid-infrared, far-infrared and submillimeter wavelengths [3, 4].

Contrary to the belief that early-type galaxies are “red and dead” with little interstellar medium and star formation [5, 6], recent studies have revealed that more than 30% of nearby early-type galaxies are rich in molecular clouds, gas and dust [7, 8, 9] due to past merger events that contribute to interstellar and nuclear activities.

NGC 1316 (Fornax A, PKS 0320-37, Arp 154) is a peculiar dusty early-type radio galaxy located in the outskirts of the Fornax cluster, at an adopted distance of 22.7 Mpc [10]. It is one of the two most luminous galaxies in the Fornax cluster and the third most powerful nearby radio source besides Centaurus A and Virgo A. It has a pair of radio lobes lying outside the optical galaxy [11] and a two-sided radio jet in the central 30'' [12]. The galaxy has a disturbed outer morphology with numerous loops, ripples, tidal tails and shells [13, 14, 15]. Spectroscopy of the brightest globular clusters suggests that a major merger took place in the galaxy about 3 Gyr ago [16] to result in the disturbed optical morphology. Other studies [14, 17] peg a merger event at about 0.5 Gyr ago. The abundance of molecular gas and misalignment between the central stellar and gas kinematics [18, 19] support a recent merger with a companion gas-rich galaxy.

NGC 1316 has prominent dust patches in the central 2'.4 x 2'.4, with an inner dust lane of about 2' oriented along the apparent optical minor axis at a position angle of  $\sim 140^\circ$  [20, 21]. Massive dust-heating stars are being formed in the galaxy [22]. The amount of dust estimated from optical extinction measurement is  $2.13 \times 10^5 M_\odot$  and that from IRAS total flux densities is  $2.11 \times 10^6 M_\odot$  [23]. The dust mass measured from the integrated Spitzer/MIPS flux densities at 24, 70 and 160  $\mu\text{m}$  is  $(2.4 \pm 0.9) \times 10^7 M_\odot$  [21, 24]. This value is consistent with the model prediction of  $3.2 \times 10^7 M_\odot$  by Draine et al. [25] at the same distance [10]. CO emission has been detected in two regions ( $\sim 30''$  southeast and  $\sim 45''$  northwest of the nucleus) with corresponding molecular hydrogen masses of  $0.9 \times 10^8 M_\odot$  and  $2.2 \times 10^8 M_\odot$  respectively [18]. X-ray observations in the energy range 0.3-8.0 keV have revealed a low-luminosity ( $L_X \sim 5.0 \times 10^{39} \text{erg s}^{-1}$ ) AGN in the galaxy [27, 28, 29].

## 2. Observations and Data Processing

NGC 1316 was observed in June 2012 for 8 hours and 10 minutes with LABOCA (Large APEX Bolometer CAmera: [31]), a bolometer camera operating on the APEX (Atacama Pathfinder EXperiment: [32]) 12 m submillimeter telescope at 5105 m elevation in the Atacama desert in Chile, one of the driest places on Earth. LABOCA observes in the continuum at a central wavelength of 870  $\mu\text{m}$  (345 GHz) in total-power scanning observing mode. The angular resolution is 19.''5 and the field of view is 11.'4. Its passband has a full width half maximum of about 60 GHz ( $\sim 150 \mu\text{m}$ ) to match the corresponding atmospheric window. The version 2.12-2 of **Crush-2** [33] was used to reduce the data and produced the full and detailed map of the dust. **Crush-2** is a comprehensive bolometric data reduction utility and imaging software package for ground-based telescopes. Iteratively, **Crush-2** removed correlated noise from the raw data in the digitized time-streams, identified and flagged problematic data pixels and provided clean and independent bolometer signals in the individual ( $\sim 70$ ) scans, which were then co-added to produce the final maps. The flux measurement, signal-to-noise ratio and the root-mean-square analyses and estimations were all done with **Crush-2**.

WISE (Wide-field Infrared Survey Explorer: [34]) is a space infrared telescope that mapped the whole sky in four mid-infrared bands at central wavelengths of 3.4, 4.6, 12 and 22  $\mu\text{m}$  labelled *W1* to *W4*. The angular resolutions are 6.1, 6.4, 6.5 and 12'' respectively. The WISE All-sky Data Products and Atlas Images are archived by the NASA IPAC (Infrared Processing and Analysis Center) in the IRSA (Infra-Red Science Archive). The reduced WISE Atlas images of NGC 1316 in the four bands were extracted from this database. The **ellipse** task in IRAF (Image Reduction and Analysis Facility) isophote package was used to determine the flux information in the respective WISE bands following the guidelines provided by the WISE Explanatory Supplement [35, 36].

### 3. Results and Discussion

As one moves to longer wavelengths ( $\lambda > 2\mu\text{m}$ ), stars contribute less and less to the observed emission, and the dust component begins to dominate. The *W1* and *W2* bands (3.4 and 4.6  $\mu\text{m}$ ) are near extinction-free bands that are mostly sensitive to the stellar population: the Rayleigh-Jeans part of the black-body emission of cool stars ( $T > 2000$  K). The emission in *W3* (12  $\mu\text{m}$ ) is dominated by PAHs (polycyclic aromatic hydrocarbons) at 11.3  $\mu\text{m}$  and warm continuum dust emission. The *W4* band (22  $\mu\text{m}$ ) is more sensitive to the warm dust emission, which comes from photon-dominated regions (or UV radiation fields) in the ambient ISM. LABOCA, at 870  $\mu\text{m}$ , is sensitive to cold dust.

#### 3.1. Flux measurements

The measured fluxes are given in Table 1. The values measured in the four WISE bands are comparable to those measured in the respective Spitzer bands (at 3.6, 4.5, 8 and 24  $\mu\text{m}$ ) for our chosen elliptical apertures. The WISE flux measurements were obtained by performing elliptical aperture photometry with the `ellipse` task in IRAF isophote package to get the total counts in each band (in data number (DN) units) after background subtractions and the respective band corrections [34, 35]. The associated errors were estimated from the corresponding uncertainty maps [36]. The measured flux in each WISE band came from an ellipse centered on the physical center (03h 22m 41.7s,  $-37^\circ 12' 30''$ ) of the image. Both the ellipticities and position angles were left to vary during the elliptical isophotal fits. The LABOCA flux was measured in a circular aperture of about  $2'$  radius.

#### 3.2. Dust maps

We used the software `Galfit` [37] to identify the stellar component. We perform a two-dimensional fit of the superposition of a Sersic model, a point-source and the sky background to the *W1* image, following the same method as [21] in their analysis of Spitzer images. Then we fixed all the parameters of the Sersic model except the amplitude, and did a fit to obtain the *W3* map. Figure 1 shows the *W3* image (*Left*) and the residual dust map (*Right*). LABOCA dust contour maps are shown in Figure 2.

**Table 1.** Flux measurements. The first column lists the four WISE bands and LABOCA with their corresponding central wavelengths in parentheses. The WISE fluxes were measured in elliptical isophotal fits using the `ellipse` task in IRAF. The semi-major axis (SMA) lengths, axis ratios and position angles are given in columns 2, 3 and 4. The total counts in each elliptical aperture were converted into integrated fluxes, given in column 5, after extended aperture corrections [35, 36]. The errors in the PA reported here are mainly statistical. The LABOCA flux was estimated in a circular aperture of about radius  $2'$  [33].

Band	SMA (arcsec)	Axis ratio	PA (deg)	Flux (Jy)
<i>W1</i> (3.4 $\mu\text{m}$ )	240.0	0.762	$50.36 \pm 0.65$	$1.968 \pm 0.031$
<i>W2</i> (4.6 $\mu\text{m}$ )	240.0	0.765	$49.54 \pm 0.71$	$1.091 \pm 0.018$
<i>W3</i> (12 $\mu\text{m}$ )	92.5	0.755	$48.09 \pm 0.63$	$0.344 \pm 0.007$
<i>W4</i> (22 $\mu\text{m}$ )	92.5	0.772	$47.35 \pm 0.58$	$0.335 \pm 0.006$
LABOCA (870 $\mu\text{m}$ )	130.0	1.000	–	$0.113 \pm 0.015$

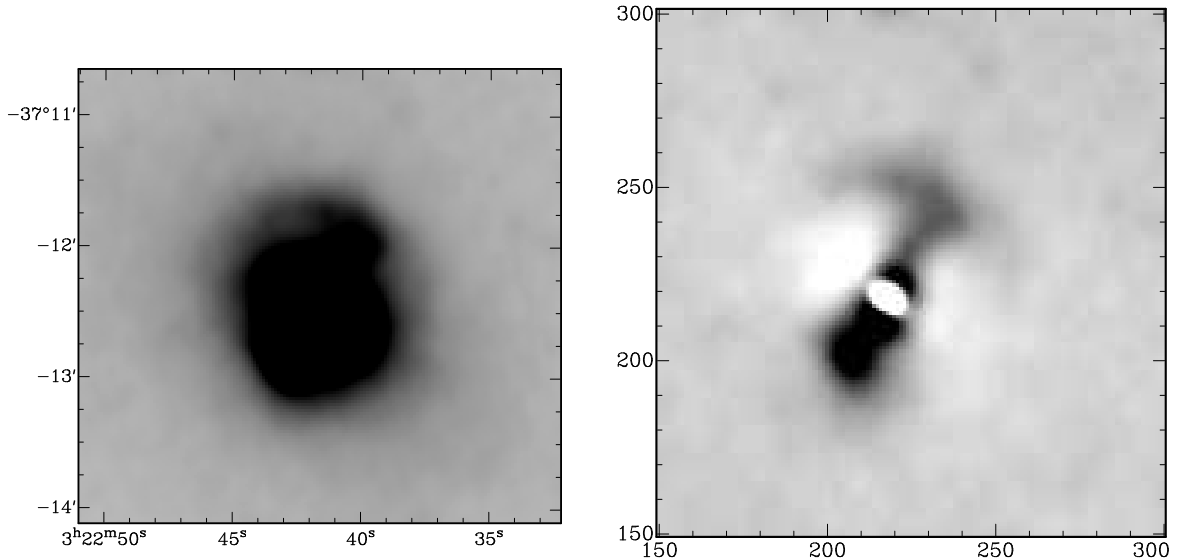


**Figure 1.** *Left:* W3 ( $12\ \mu\text{m}$ ) map of NGC 1316. *Right:* Preliminary W3 dust map obtained after subtraction of the stellar component modeled as a Sersic model and of a central position source. The northern dusty “arc” and the southern dust concentration seen in the HST and in Spitzer images [21] are apparent. The width of the image is about  $3.''45$  (150 pixels of  $1.''375$ ).

### 3.3. Spectral energy distribution

We did a fit to published mid-infrared flux measurements from the literature and to our LABOCA submillimeter measurement, to model the SED of NGC 1316, as shown in Figure 3. We modeled the dust emission as the superposition of two modified black-body components at different temperatures,

$$S_\nu = A_w \lambda^{-\beta_w} B_\nu(T_w) + A_c \lambda^{-\beta_c} B_\nu(T_c) \quad (1)$$

where  $\beta_w$  and  $\beta_c$  are the dust emissivity indices for the respective warm ( $T_w$ ) and cold ( $T_c$ ) temperature components. We fixed the emissivity indices to 2.  $B_\nu(T)$  is the Planck function at the temperature of interest,  $A_w$  and  $A_c$  are amplitudes [26]. The inferred temperature values are  $T_w = 55.0 \pm 4.2$  K and  $T_c = 21.7 \pm 1.3$  K, in agreement with previous estimates.

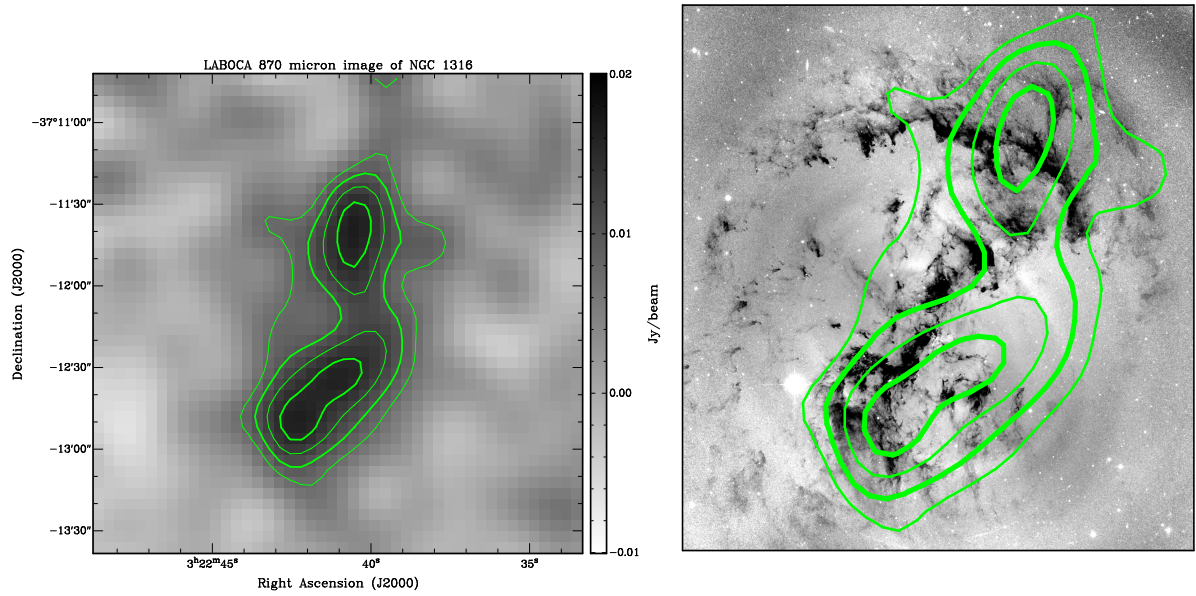


**Figure 2.** *Left:* LABOCA 870  $\mu\text{m}$  image of NGC 1316 in greyscale and contours. The contours range from 3 to 6 times the noise level, which is equal to 2.5 mJy/beam. The angular resolution of the image is  $28''$ . *Right:* HST image in greyscale and LABOCA image in contours. The two peaks detected in the submillimeter map correspond roughly to the dust lanes seen in extinction in the HST image.

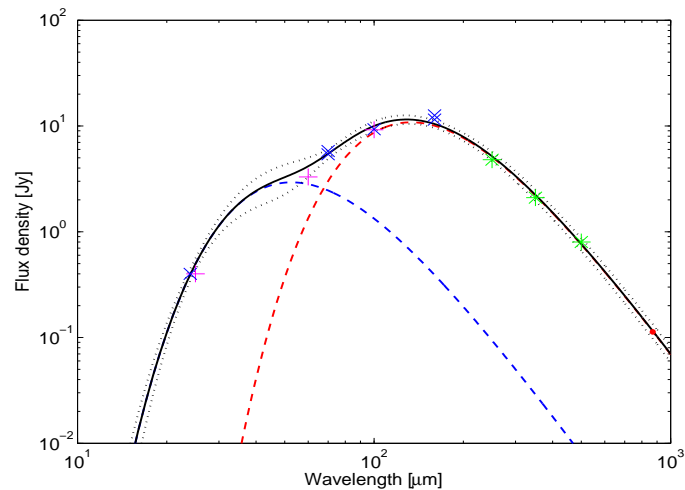


**Figure 3.** Mid-infrared to submm spectral energy distribution of NGC 1316. The points are the measurements listed in Table 2 of [26] and our LABOCA point shown in red. The magenta pluses are from IRAS, the blue crosses from Spitzer, the green stars from Herschel. The dashed lines show the best-fit models of the cold dust emission (in red) and the warm dust emission (in blue). The black solid line is the sum of the two, and the dotted lines show the 95% confidence interval. The emissivity index was fixed to 2 for both components.

#### 4. Conclusion

We have presented an ongoing analysis of the dust emission in the galaxy NGC 1316 based on WISE and LABOCA measurements in the mid-infrared and in the submillimeter. The separation of the stellar component from the dust is crucial and will be refined. In the future, we plan to use all available maps to infer resolved SEDs, following the work of Galametz et al. 2012 [26] and including long-wavelength data. NGC 1316 is a target of choice for future observations of the dust and molecular gas with ALMA (Atacama Large Millimeter/submillimeter Array) to study their possible interaction with the inner radio jet.

#### 5. Acknowledgements

We thank Zolt Levay and Paul Goudfrooij for making their HST image available to us. The first author wishes to thank Tom H. Jarrett for the initial guide on WISE flux measurement.

#### References

- [1] Spitzer L 1978 *Physical Processes in the Interstellar Medium* (New York: Wiley) pp 250–333
- [2] Blain A W, Smail I, Ivison R J, Kneib J P and Frayer D T 2002 *Phys Reports* **369** 111
- [3] Draine B T 2009 *Space Sci. Revs.* **143** 333–45
- [4] Kennicutt R C et al. 2003 *Publ. Astron. Soc. Pac.* K **115** 928–52
- [5] Faber S M and Gallagher J S 1976 *Astrophysical J.* **204** 356
- [6] Thomas D, Maraston C, Bender R and Mendes de Oliveira C 2005 *Astrophysical J.* **621** 673–94
- [7] Leeuw L L, Davidson J, Dowell C D and Matthews H E. 2008 *Astrophysical J.* **677** 249
- [8] Kuntschner H et al. 2010 *Mon. Not. R. Astron. Soc.* **408** 97–132
- [9] Bureau M et al. 2011 *IAU Symposium* **277** 55–8
- [10] Tonry J L et al. 2001 *Astrophysical J.* **546** 681
- [11] Ekers R D, Goss W M, Wellington K J, Bosma A, Smith R M and Schweizer F 1983 *A & A* **127** 361–65
- [12] Geldzahler B J and Fomalont E B 1984 *Astronomical J.* **89** 1650–57
- [13] Schweizer F and Seitzer P 1988 *Astrophysical J.* **328** 88
- [14] Schweizer F 1980 *Astrophysical J.* **237** 303–18
- [15] Matthews T A, Morgan W W and Schmidt M 1964 *Astrophysical J.* **140** 35
- [16] Goudfrooij P, Gilmore D, Whitmore B C and Schweizer F 2004 *Astrophysical J.* **613** 121
- [17] Mackie G and Fabbiano G 1998 *Astrophysical J.* **115** 514
- [18] Horellou C, Black J H, van Gorkom J H, Combes F, van der Hulst J M and Charmandaris V 2001 *A & A* **376** 837–52
- [19] Bosma A, Smith R M and Wellington K J 1985 *Mon. Not. R. Astron. Soc.* **212** 301
- [20] Grillmair C J, Forbes D A, Brodie J P and Elson R A W 1999 *Astronomical J.* **117** 167–80
- [21] Lanz L, Jones C, Forman W R, Ashby M L N, Kraft R and Hickox R 2010 *Astrophysical J.* **721** 1702–13
- [22] Temi P, Mathews W G and Brighenti F 2005 *Astrophysical J.* **622** 235–43
- [23] Deshmukh S P, Tate B T, Vagshette N D, Pandey S K and Patil M K 2012 A multiwavelength view of the ISM in the merger remnant Fornax A galaxy *eprint* arXiv:1207.4324
- [24] Dale D A et al. 2007 *A & A D* **655** 863–84
- [25] Draine B T et al. 2007 *Astrophysical J.* **663** 866–94
- [26] Galametz M et al. 2012 *Mon. Not. R. Astron. Soc.* **425** 763
- [27] Kim D W and Fabbiano G 2003 *Astrophysical J.* **586** 826
- [28] Feigelson E D, Laurent-Muehleisen S A, Kollgaard R I and Fomalont E B 1995 *Astrophys. J. Lett.* **449** 149
- [29] Fabbiano G, Kim D W and Trinchieri G 1992 *Astrophysical J. Suppl. Ser.* **80** 531–644
- [30] Hopkins P F and Quataert E 2010 *Mon. Not. R. Astron. Soc.* **407** 1529
- [31] Siringo G et al. 2009 *A & A D* **497** 945–62
- [32] Güsten R, Nyman L A, Schilke P, Menten K, Cesarsky C and Booth R 2006 *A & A* **497** 13
- [33] Kovács A 2008 *SPIE Proc.* **7020** 45K
- [34] Wright E L et al. 2010 *Astronomical J.* **140** 1868–81
- [35] Jarrett T H et al. 2013 *Astronomical J.* **145** 1–34
- [36] Cutri R M et al. 2012 *WISE All-Sky Data Release Products Explanatory Supplement 2012wise report.*
- [37] Peng C Y, Ho L C, Impey C D and Rix H 2002 *Astronomical J.* **124** 226